

# Uncertainty Analysis of Ferroelectric Polydomain Structures

Paul Miles

Department of Mathematics, North Carolina State University

Authors: Paul Miles<sup>a</sup>, William Oates<sup>b</sup>, Lider Leon<sup>a</sup>, Ralph Smith<sup>a</sup>

<sup>a</sup>Department of Mathematics, North Carolina State University

<sup>b</sup>Department of Mechanical Engineering, Florida Center for Advanced Aero-Propulsion (FCAAP),  
Florida A&M and Florida State University

Support:

<sup>a</sup> NSF Grant CMMI-1306290 Collaborative Research CDS&E

<sup>b</sup> NSF Grant CMMI-1306320 Collaborative Research CDS&E

# Materials: Ferroelectrics

- Applications:
  - Energy harvesting
  - Structural health monitoring
  - Flow control
  - Ultrasound
  - Robotics
  - Sonar
  - Nanopositioning



Figure: Piezoelectric ceramics are mechanically deformed when in the presence of an electric field. The reverse mechanism is also true, in that an electrical response is generated if a mechanical load is applied.

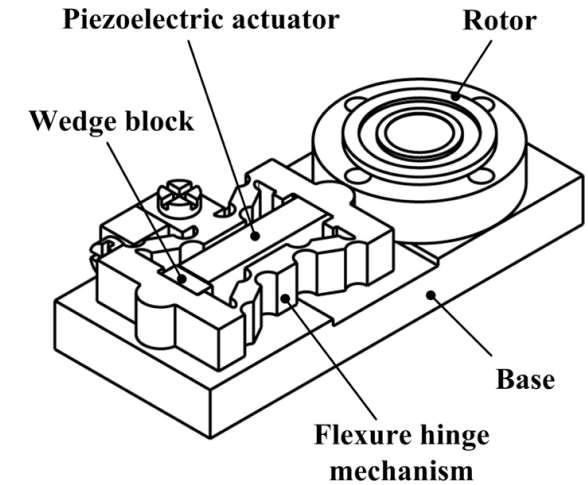


Figure: Schematic of nanoposition stage<sup>1</sup>.

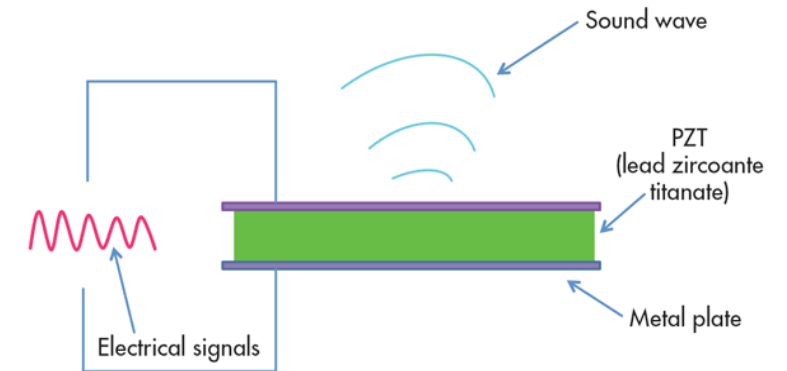


Figure: Schematic of piezoelectric in sonar transducer<sup>2</sup>.

1. Li, Jianping, et al. "Design and experimental tests of a dual-servo piezoelectric nanopositioning stage for rotary motion." *Review of Scientific Instruments* 86.4 (2015): 045002.  
2. <http://www.electronicdesign.com/power/what-piezoelectric-effect>

# Polydomain Structures

- Atomic structure broken up into domains
  - Domains – regions of uniform polarization
- Domains divided by walls
  - Most active material behavior occurs along domain wall
  - Extending work done by Cao & Cross<sup>1</sup> and Meyer & Vanderbilt<sup>2</sup>.

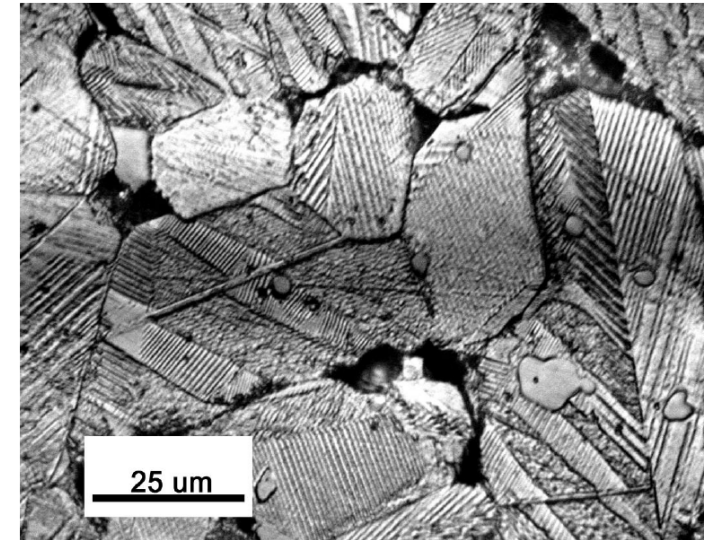


Figure: Domain structures in Barium Titanate<sup>3</sup>.

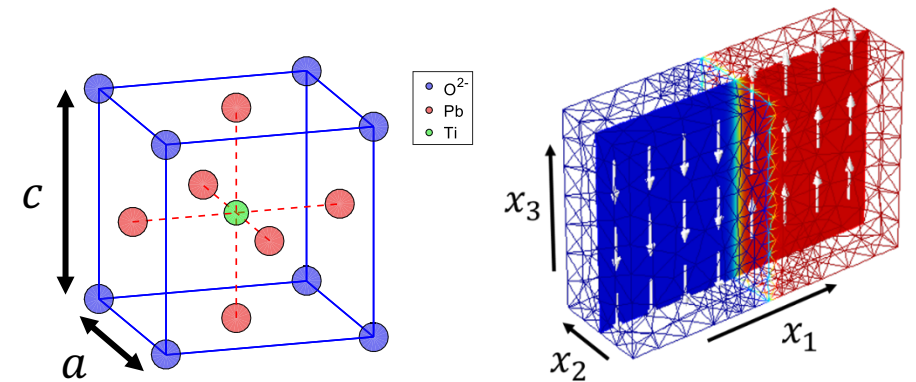


Figure: (Left) Unit cell width is approximately 4 angstroms. (Right) Domains separated by walls that are approximately 5 angstroms wide.

1. Cao, W., and Cross, L.E. "Theory of Tetragonal Twin Structures in Ferroelectric Perovskites with a First-Order Phase Transition." *Physical Review B* 44.1 (1991)  
2. Meyer, B., and Vanderbilt, D. "Ab initio study of ferroelectric domain walls in  $PbTiO_3$ ". *Physical Review B*, 65(10):104111, 2002.  
3. Liang, D., Stone, D., and Lakes, R. "Softening of bulk modulus and negative Poisson ratio in barium titanate ceramic near the Curie point." *Philosophical Magazine Letters* 90.1 (2010): 23-33.

# Polydomain Structures

## 180° Domain Wall

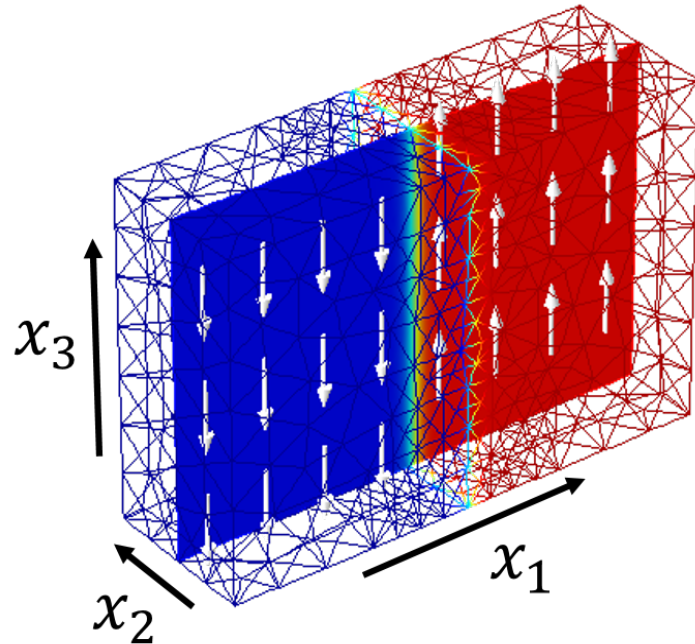


Figure: 180° domain wall – two distinct polarization regions. On the left (blue) we have polarization in the negative  $x_3$  direction and on the right (red) the polarization is in the positive  $x_3$  direction. The polarization switches by 180° as you pass through the domain wall.

## 90° Domain Wall

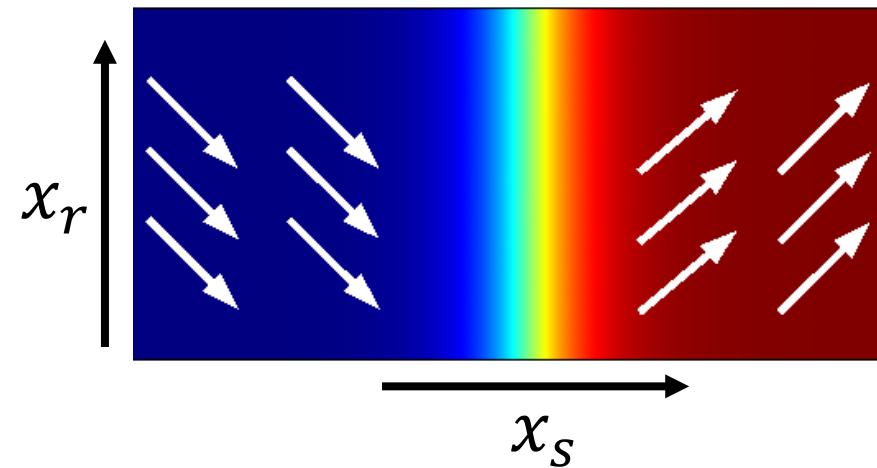


Figure: 90° domain wall – two distinct polarization regions. On the left (blue) we have polarization with components in the positive  $x_1$ -direction and negative  $x_2$ -direction. On the right (red) the polarization is in the positive  $x_1$ - and  $x_2$ -direction. The polarization switches by 90° as you pass through the domain wall.

# Continuum Model

---

- Free energy density

$$u(P_i, P_{i,j}, \varepsilon_{ij}) = u_M(\varepsilon_{ij}) + u_L(P_i) + u_C(P_i, \varepsilon_{ij}) + u_G(P_{i,j})$$

- Components

$u_M$  - elastic energy

$u_L$  - Landau energy

$u_C$  - electrostrictive energy

$u_G$  - polarization gradient energy

$P_i$  - polarization in  $i^{th}$  direction

$P_{i,j}$  - polarization gradient

$\varepsilon_{ij}$  - strain

# Continuum Model: Monodomain Structures

---

$$\text{Energy: } u(P_i, \varepsilon_{ij}) = u_M(\varepsilon_{ij}) + u_L(P_i) + u_C(P_i, \varepsilon_{ij})$$

$$\text{Stress: } \sigma_{ij} = \left( \frac{\partial u}{\partial \varepsilon_{ij}} \right)$$

$$u_L(P_i) = \alpha_1 (P_1^2 + P_2^2 + P_3^2) + \alpha_{11} (P_1^2 + P_2^2 + P_3^2)^2 \\ + \alpha_{12} (P_1^2 P_2^2 + P_2^2 P_3^2 + P_1^2 P_3^2) + \dots$$

$$u_C = -q_{11} (\varepsilon_{11} P_1^2 + \varepsilon_{22} P_2^2 + \varepsilon_{33} P_3^2) \\ - q_{12} [\varepsilon_{11} (P_2^2 + P_3^2) + \varepsilon_{22} (P_1^2 + P_3^2) + \varepsilon_{33} (P_1^2 + P_2^2)] \\ - q_{44} (\varepsilon_{12} P_1 P_2 + \varepsilon_{13} P_1 P_3 + \varepsilon_{23} P_2 P_3)$$

# Uncertainty Quantification: Bayesian Statistical Analysis

---

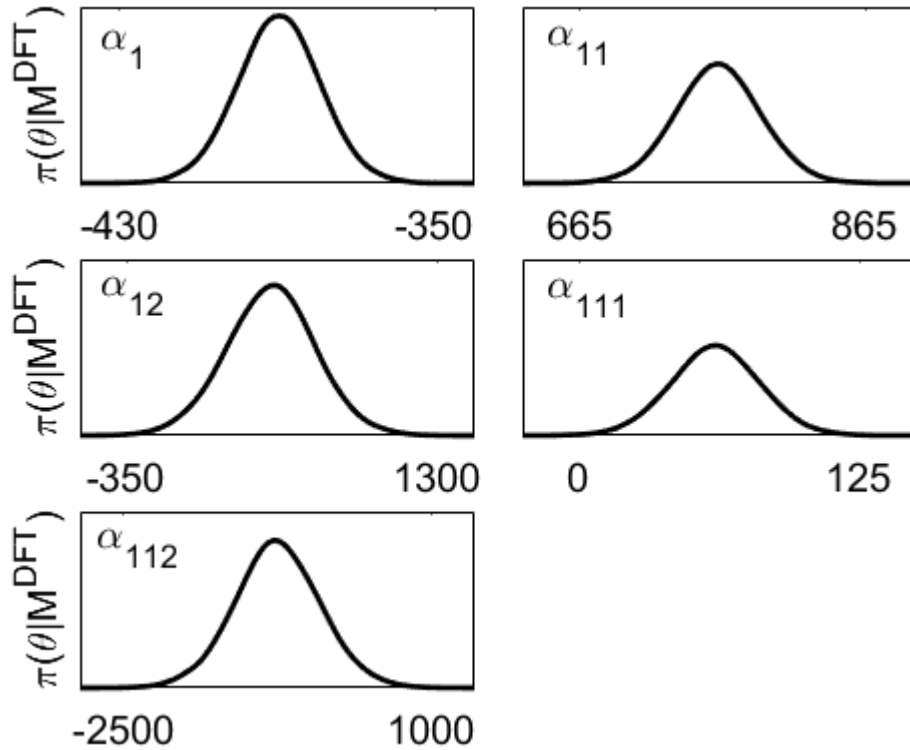
- Statistical Model:  $M^{data}(i) = M(i; \theta) + \varepsilon_i, \quad i = 1, \dots, N$
- Bayes' Relation

$$\pi(\theta | M^{data}) = \frac{p(M|\theta)\pi_0(\theta)}{\int_{\mathbb{R}^p} p(M|\theta)\pi_0(\theta)d\theta}$$

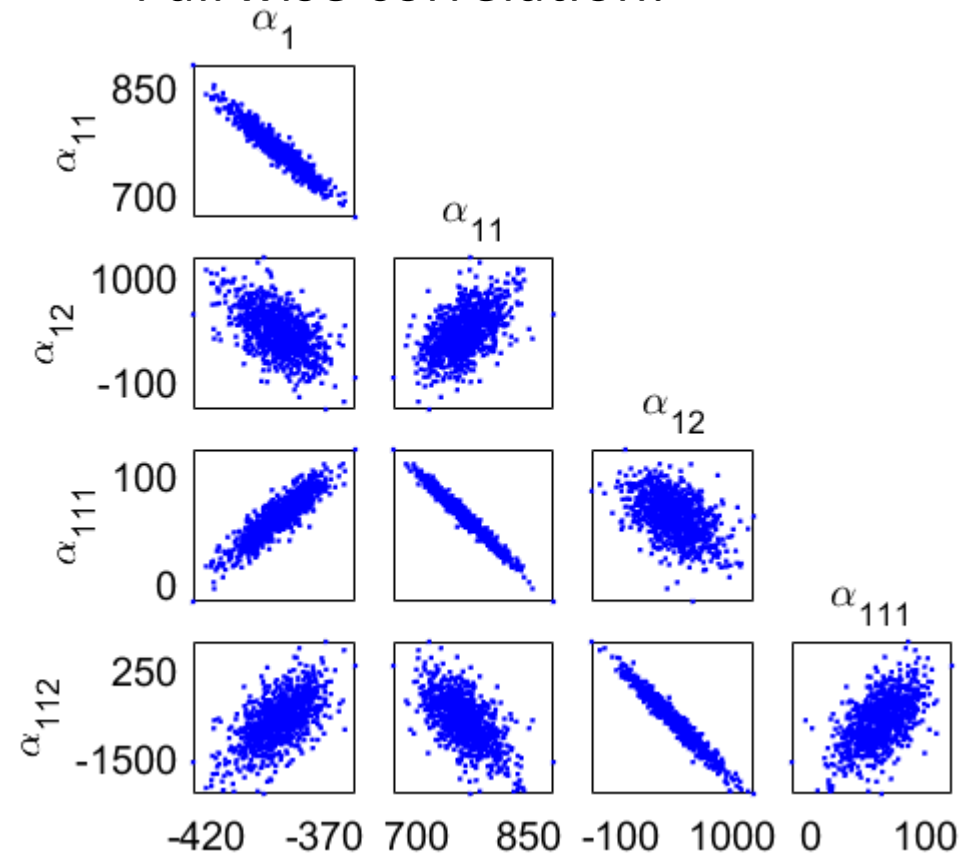
- Posterior Density:  $\pi(\theta | M^{data})$
- Prior Density:  $\pi_0(\theta)$
- Likelihood Function:  $p(M|\theta) = e^{-\sum_{i=1}^n [M^{data}(i) - M(i;\theta)]^2 / (2\sigma^2)}$ 
  - Assume observation errors are independent and identically distributed (iid):  $\varepsilon_i \sim N(0, \sigma^2)$ .

# Uncertainty Quantification: Monodomain Structures

- Posterior densities:  $\pi(\theta|M^{data})$



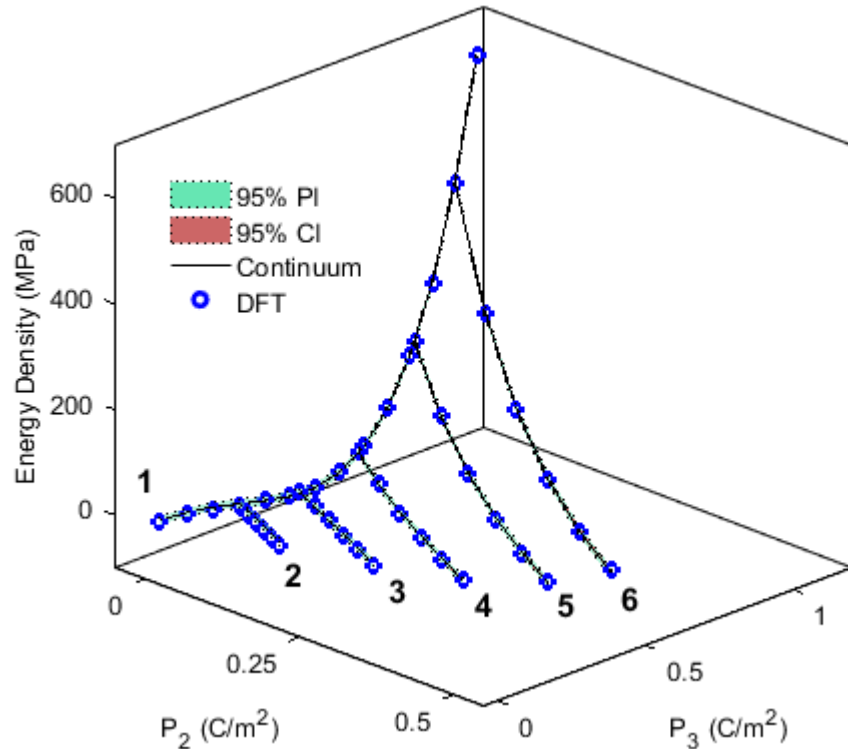
- Pairwise correlation:





# Uncertainty Propagation: Monodomain Structures

- Energy density:  $u$



- Stress:  $\sigma_{11}$

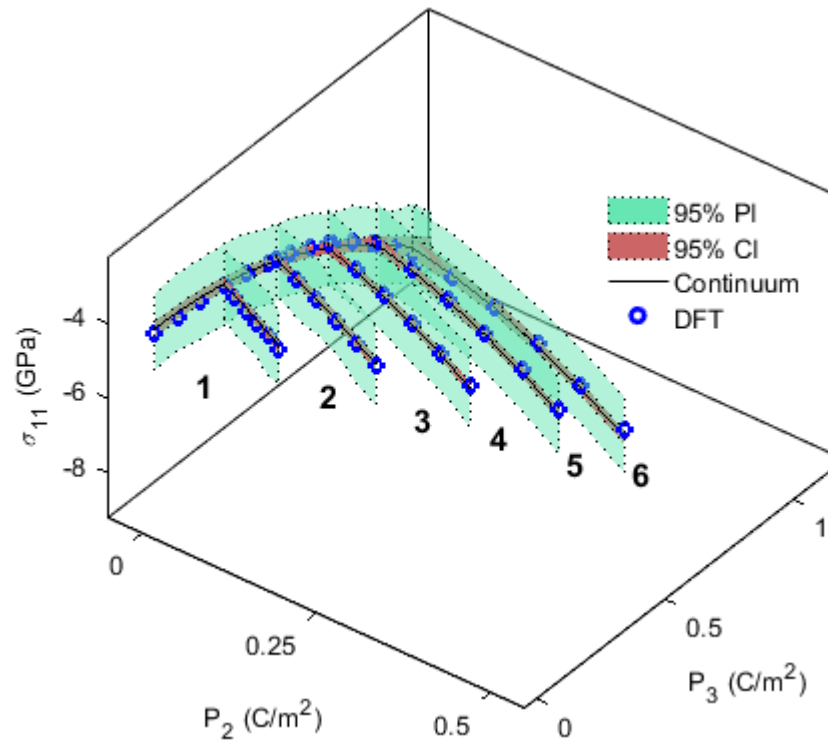


Figure: (Left) Uncertainty propagation through energy model and (Right) uncertainty in normal stress in the  $x_1$  direction.

# Continuum Model: Polydomain Structures

---

- Governing equations

$$\text{Ginzburg-Landau: } \frac{d}{dx_j} \left( \frac{\partial u}{\partial P_{i,j}} \right) - \frac{\partial u}{\partial P_i} = 0$$

$$\text{Momentum: } \sigma_{ij,j} = \frac{d}{dx_j} \left( \frac{\partial u}{\partial \varepsilon_{ij}} \right) = 0$$

- Gradient energy

$$u_G = \frac{g_{11}}{2} (P_{1,1}^2 + P_{2,2}^2 + P_{3,3}^2) + g_{12} (P_{1,1}P_{2,2} + P_{1,1}P_{3,3} + P_{2,2}P_{3,3}) \\ + \frac{g_{44}}{2} \left[ (P_{1,2} + P_{2,1})^2 + (P_{1,3} + P_{3,1})^2 + (P_{2,3} + P_{3,2})^2 \right]$$

# Continuum Model: 180° Domain Wall

- Assume:

$P_1 = P_2 = 0, P_3 \neq 0, \varepsilon_{ij} = 0 (i \neq j)$ , and only spatial variation is in  $x_1$ -direction

- Ginzburg-Landau:

$$\frac{\partial}{\partial x_1} \left( \frac{\partial u}{\partial P_{3,1}} \right) - \frac{\partial u}{\partial P_3} = 0 \rightarrow 2\alpha_1^+ P_3 + 4\alpha_{11} P_3^3 + 6\alpha_{111} P_3^5 = g_{44} P_{3,1}$$

where  $\alpha_1^+ = \alpha_1 - q_{11}\varepsilon_{33} - q_{12}(\varepsilon_{11} + \varepsilon_{22})$

- Momentum:

$$\sigma_{11,1} = \frac{\partial}{\partial x_1} \left( \frac{\partial u}{\partial \varepsilon_{11}} \right) = c_{11}\varepsilon_{11,1} - 2q_{12}P_3P_{3,1} = 0$$

- Numerically solve for  $P_3$  and  $\varepsilon_{11}$

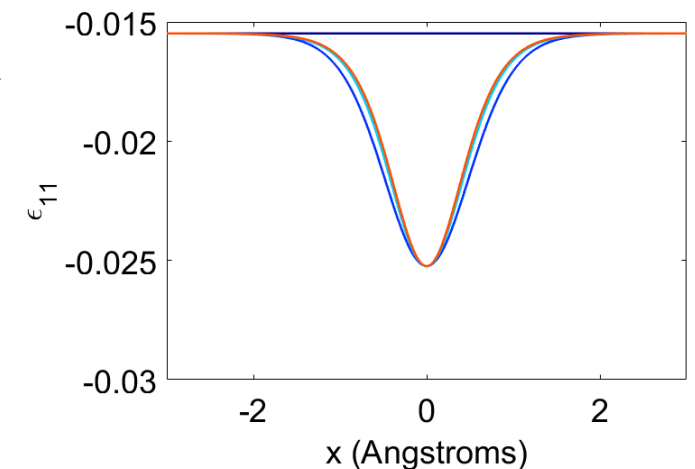
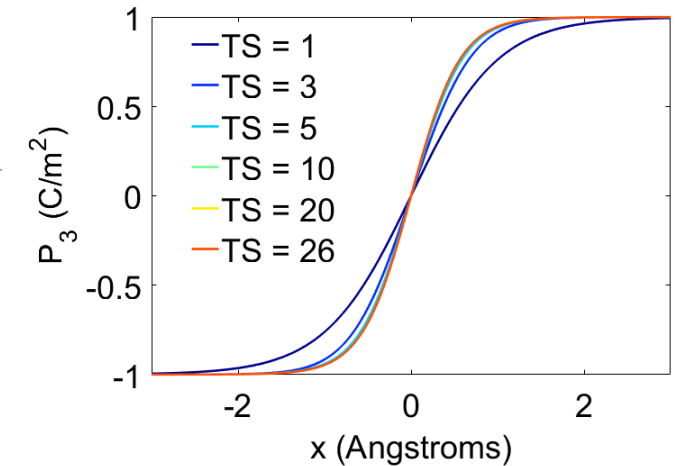


Figure: 180° domain wall numerical solution for polarization and strain. Numerical solution converges to steady state solution.

# Model Comparison: 180° Domain Wall

- Finite difference (FD)
  - Simplified model
- Finite element analysis (FEA)
  - More degrees of freedom
- Good model agreement between FD and FEA
  - Compare quantities of interest

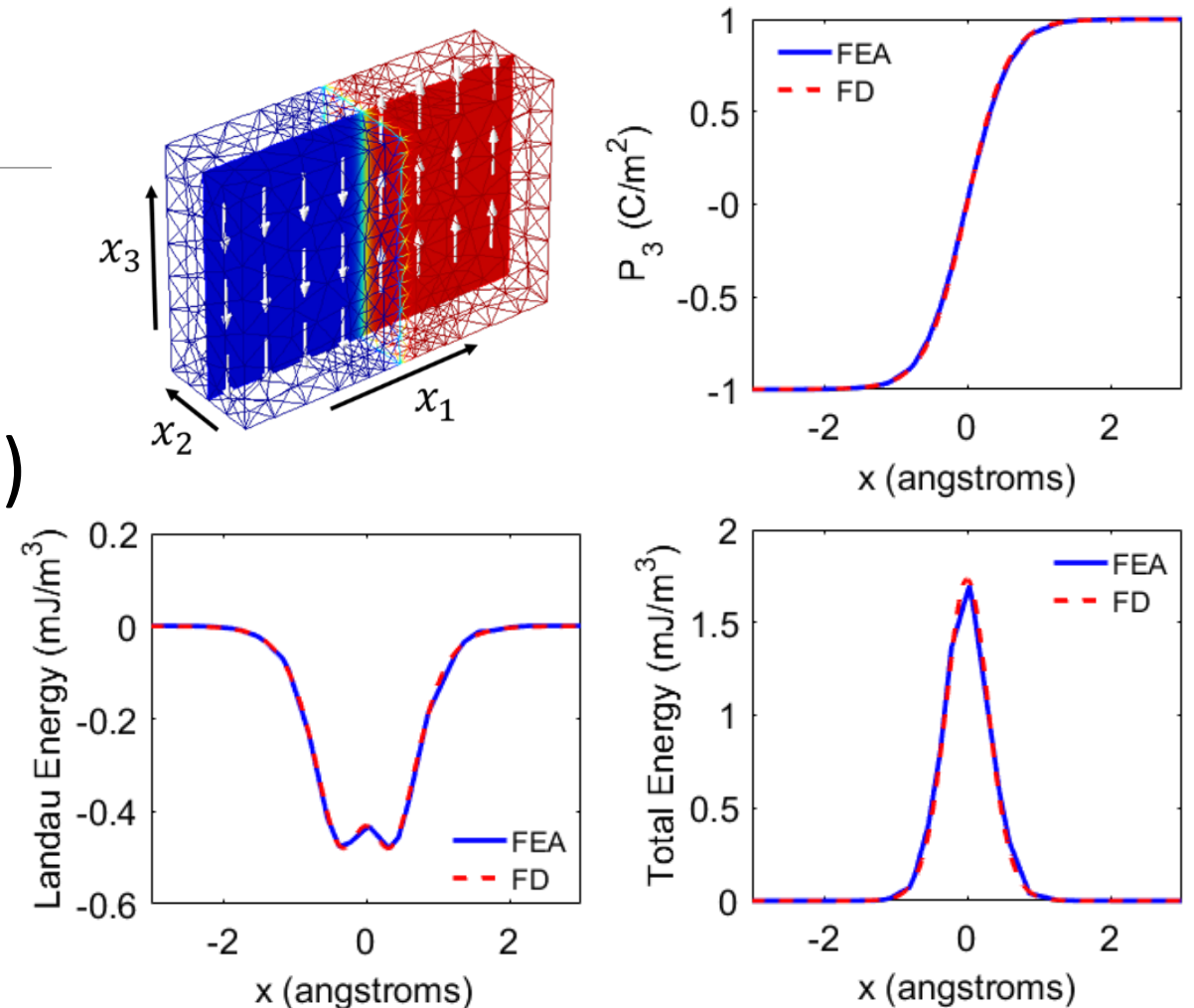


Figure: 180° domain wall energy along  $x_1$ -axis. (Top Right) Polarization switches from negative to positive within the nanoscale domain wall region. Compared solution found using FEA and FD: (Bottom Left) Landau energy density and (Bottom Right) total energy density.

# Polydomain Structures: 180° Domain Wall

- Domain wall energy

$$E_{180^\circ} = \int_{-\infty}^{\infty} (u - u_0) dx_1$$

- From literature<sup>1</sup>:  $E_{180^\circ} = 132 \text{ mJ/m}^2$

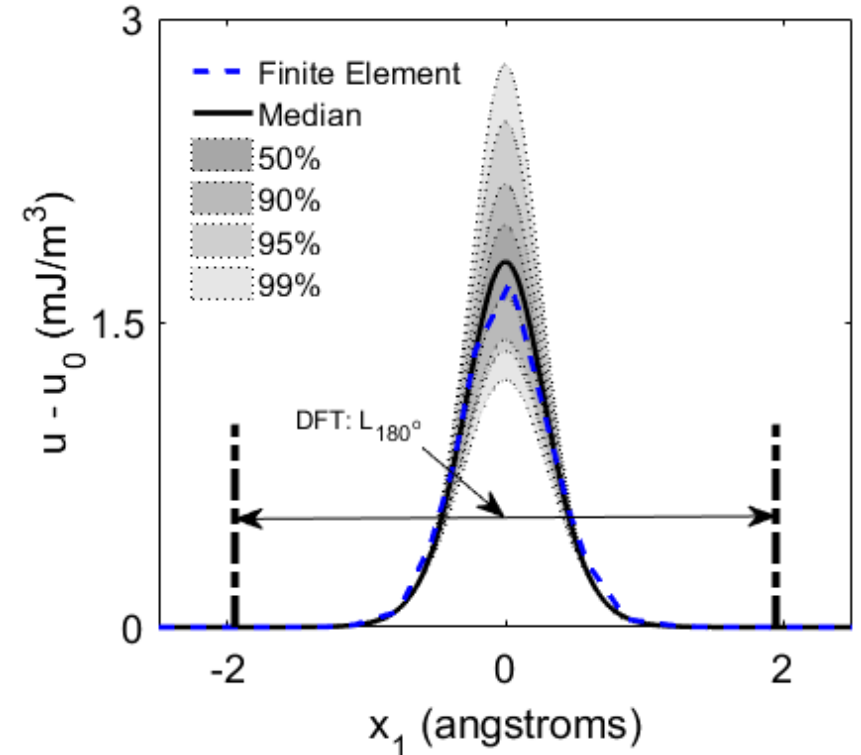
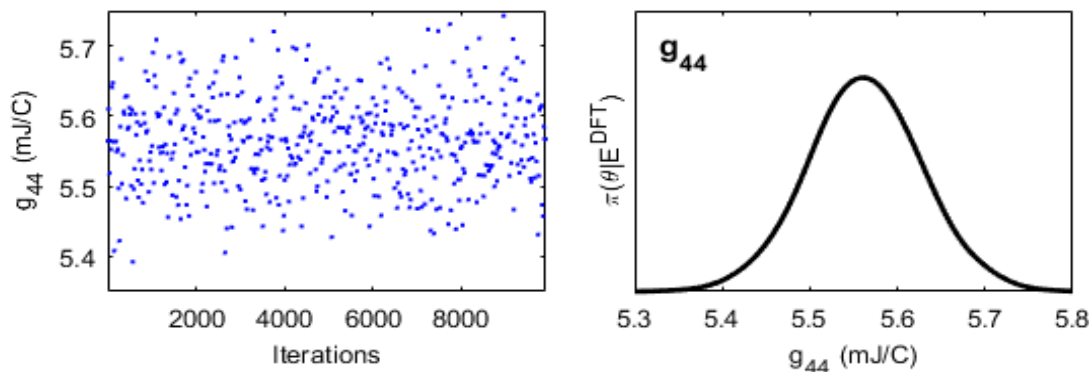
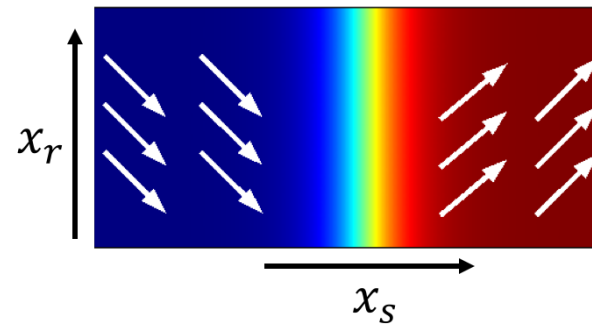


Figure: Excess energy density through 180° domain wall energy along  $x_1$ -axis. Uncertainty from continuum model parameters propagated through to generate 50% - 99% credible intervals.

1. Meyer, B., and Vanderbilt, D. "Ab initio study of ferroelectric domain walls in  $PbTiO_3$ ". Physical Review B, 65(10):104111, 2002.

# Continuum Model: 90° Domain Wall



- Easier to work in rotated coordinate system:
  - Rotate 45° degrees around the  $x_3$  axis –  $(x_s, x_r, x_3)$

- Ginzburg-Landau:

$$\frac{\partial}{\partial x_s} \left( \frac{\partial u}{\partial P_{s,s}} \right) - \frac{\partial u}{\partial P_s} = 0 \rightarrow G_{ss} P_{s,ss} = \beta_1 P_s + \beta_2 P_s^3 + \beta_3 P_s^5 + \beta_4 P_s P_r^2 + \beta_5 P_s P_r^4 + \beta_6 P_s^3 P_r^2$$

$$\frac{\partial}{\partial x_s} \left( \frac{\partial u}{\partial P_{r,s}} \right) - \frac{\partial u}{\partial P_r} = 0 \rightarrow G_{rs} P_{r,ss} = \gamma_1 P_r + \gamma_2 P_r^3 + \gamma_3 P_r^5 + \gamma_4 P_s^2 P_r + \gamma_5 P_s^4 P_r + \gamma P_s^2 P_r^3$$

where  $\beta_i, \gamma_i = f(\alpha_1, \alpha_{11}, \dots, q_{11}, \dots, c_{11}, \dots, g_{11}, \dots)$

# Conclusions & Future Work: Quantum-Informed Continuum Modeling

---

- $180^\circ$ 
  - Developed numerical approximation and verified with finite element solution
  - Quantified uncertainty associated with exchange parameter
- $90^\circ$ 
  - Developed numerical approximation
  - Ongoing effort to verify with finite element analysis

# Acknowledgements

---

## Support:

- NSF Grant CMMI-1306290 Collaborative Research CDS&E
- NSF Grant CMMI-1306320 Collaborative Research CDS&E

